Journal of Biomedical Optics

BiomedicalOptics.SPIEDigitalLibrary.org

Excitation of erbium-doped nanoparticles in 1550-nm wavelength region for deep tissue imaging with reduced degradation of spatial resolution

Masahito Yamanaka
Hirohiko Niioka
Taichi Furukawa
Norihiko Nishizawa

SPIE.

Masahito Yamanaka, Hirohiko Niioka, Taichi Furukawa, Norihiko Nishizawa, "Excitation of erbium-doped nanoparticles in 1550-nm wavelength region for deep tissue imaging with reduced degradation of spatial resolution," *J. Biomed. Opt.* **24**(7), 070501 (2019), doi: 10.1117/1.JBO.24.7.070501.

Excitation of erbium-doped nanoparticles in 1550-nm wavelength region for deep tissue imaging with reduced degradation of spatial resolution

Masahito Yamanaka,[a,*] Hirohiko Niioka,[b,*] Taichi Furukawa,[c] and Norihiko Nishizawa[a]
[a]Nagoya University, Department of Electronics, Furo-cho, Chikusa-ku, Nagoya, Aichi, Japan
[b]Osaka University, Institute for Datability Science, Suita, Osaka, Japan
[c]Yokohama National University, Faculty of Engineering, Hodogaya-ku, Yokohama, Kanagawa, Japan

Abstract. Rare-earth-doped nanoparticles are one of the emerging probes for bioimaging due to their visible-to-near-infrared (NIR) upconversion emission via sequential single-photon absorption at NIR wavelengths. The NIR-excited upconversion property and high photostability make this probe appealing for deep tissue imaging. So far, upconversion nanoparticles include ytterbium ions (Yb^{3+}) codoped with other rare earth ions, such as erbium (Er^{3+}) and thulium (Tm^{3+}). In these types of upconversion nanoparticles, through energy transfer from Yb^{3+} excited with continuous wave light at a wavelength of 980 nm, upconversion emission of the other rare earth dopants is induced. We have found that the use of the excitation of Er^{3+} in the 1550-nm wavelength region allows us to perform deep tissue imaging with reduced degradation of spatial resolution. In this excitation–emission process, three and four photons of 1550-nm light are sequentially absorbed, and Er^{3+} emits photons in the 550- and 660-nm wavelength regions. We demonstrate that, compared with the case using 980-nm wavelength excitation, the use of 1550-nm light enables us to moderate degradation of spatial resolution in deep tissue imaging due to the lower light scattering coefficient compared with 980-nm light. We also demonstrate that live cell imaging is feasible with this 1550 nm excitation. [DOI: 10.1117/1.JBO.24.7.070501]

Keywords: upconversion emission imaging; rare-earth-doped nanoparticle; erbium; 1550 nm wavelength; high-resolution.

Paper 190132LR received Apr. 29, 2019; accepted for publication Jun. 24, 2019; published online Jul. 12, 2019.

*Address all correspondence to Masahito Yamanaka, E-mail: yamanaka.masahito@h.mbox.nagoya-u.ac.jp; Hirohiko Niioka, E-mail: niioka@ids.osaka-u.ac.jp

1 Introduction

Fluorescence/luminescence imaging techniques play a key role in life sciences since they allow us to visualize structures and molecules in biological specimens with high spatial resolution and specificity. When applying these imaging techniques to the investigation of thick biological specimens, near-infrared (NIR) light is commonly used because it penetrates deeper into specimens than visible light does. One of the main NIR imaging techniques is multiphoton excited fluorescence microscopy.[1] This technique uses NIR ultrashort laser pulses to excite fluorescent probes via multiphoton absorption and then induce shorter wavelength fluorescence, which is typically in the visible wavelength region. The combination of the high penetration depth of NIR light and the localization of the multiphoton excitation volume in the laser focus offers deep tissue imaging capability with cellular-level spatial resolution, optical sectioning capability, and high image contrast. Another major approach for NIR deep tissue imaging is to use probes to bring about fluorescent/luminescent emission under single-photon excitation by NIR light. Recently, various types of NIR probes, including red/deep-red fluorescent proteins,[2,3] NIR dyes,[4] quantum dots,[4,5] carbon nanotubes,[6] and rare-earth (RE)-doped nanoparticles,[7–9] have been reported. Recent advances in the development of NIR fluorescent/luminescent probes allow NIR imaging to be performed by using simple conventional fluorescence microscopes equipped with a continuous wave (CW) NIR laser or lamp sources.

Among these NIR probes, RE-doped nanoparticles, triplet–triplet annihilation nanoparticles, and so on have the feature of converting NIR photons to shorter wavelength photons.[7–10] The use of upconversion nanoparticles (UCNPs) as probes for imaging allows us to significantly reduce autofluorescence background from the samples and optics, such as the case of multiphoton excited fluorescence microscopy. Other important benefits are that the photostability of the UCNPs is significantly higher than that of conventional fluorescent dyes,[8] and it is not necessary to use high-intensity ultrashort-pulse laser sources such as those used for multiphoton excited fluorescence microscopy, because the upconversion emission is induced via sequential single-photon absorption.

RE-doped UCNPs are usually produced by using host materials such as Y_2O_3 or $NaYF_4$.[7–9] In host materials, several kinds of rare-earth ions such as ytterbium (Yb^{3+}), erbium (Er^{3+}), and thulium (Tm^{3+}) are codoped. To induce upconversion luminescence emission, Yb^{3+} is excited by 980-nm CW light and then energy transfer from Yb^{3+} leads to upconversion emission of other rare earth dopants in a shorter wavelength region. Recently, there has been a wide variety of reports on the development of brighter and functional UCNPs using rare earth ions with 980-nm excitation and the use of RE-doped UCNPs for studies in life science.[11,12]

In this letter, we report that using the excitation of Er^{3+}-doped nanoparticles in the 1550-nm wavelength region allows us to perform deep tissue imaging with reduced degradation of spatial resolution. Although the upconversion photoluminescence properties of Er^{3+}-doped phosphors under 1550-nm excitation have been already studied previously,[13,14] the imaging properties in using the 1550-nm excitation of Er^{3+}-doped nanoparticles remain unclear. In deep tissue imaging, the spatial resolution is degraded due to a variety of reasons, including optical aberrations, light scattering, and so on. Compared with 980-nm light, 1550-nm light has a smaller scattering coefficient.[15]

Therefore, it is expected that the use of excitation light with a smaller scattering coefficient will moderate the degradation of the spatial resolution in deep tissue imaging. In the NIR wavelength region, it has been reported that there are four NIR optical tissue windows where high penetration depth is achieved in imaging turbid scattering tissue (first: 650 to 950 nm, second: 1000 to 1350 nm, third: 1550 to 1850 nm, and fourth: centered at 2200 nm).[3,15] The wavelength of 1550 nm is in the third NIR optical tissue window. In this work, to confirm the moderated degradation of the spatial resolution by using 1550-nm light, we demonstrated luminescence imaging of Er^{3+}-doped nanoparticles through a skin tissue phantom. In addition, we also performed live cell imaging by introducing Er^{3+}-doped nanoparticles into HeLa cells through endocytosis. In our experiments, to compare luminescence images of the same nanoparticles under 980 and 1550 nm excitation, we used $NaYF_4$: Er, Yb nanoparticles with diameters of 10 to 60 nm (74344, Sigma Aldrich), which can be excited at both wavelengths.

2 Upconversion Emission Spectrum and Luminescence Responses

To confirm the wavelengths of the upconversion emission of $NaYF_4$: Er, Yb nanoparticles excited by 1550-nm light, we measured their luminescence spectrum. We fixed the nanoparticles on a coverslip and immersed them in water. For the measurement, we used our custom-built inverted laser-scanning microscope equipped with a 1550-nm CW laser source (FPL1009S, Thorlabs). The 1550-nm light was focused onto nanoparticles with a 1.05 NA silicone-immersion objective lens (UPLSAPO30XSIR, Olympus), and the emitted luminescence was collected with the same objective lens. This objective lens had an optical transmittance of ~80% in the 400- to 1600-nm wavelength region. The emission spectrum was recorded with a fiber-coupled spectrometer (USB2000, Ocean Optics). As shown in Fig. 1(a), we confirmed that the upconversion emission had two peaks in the 550- and 660-nm wavelength regions.

We also evaluated the relationship between the luminescence and excitation intensities. To induce the luminescence emission of Er^{3+} in the 550- and 660-nm wavelength regions by 1550-nm excitation, three and four photons in the 1550-nm wavelength are required, and the possible UC mechanism is described in Refs. 16 and 17. Because these are three- and four-photon absorption processes, it was expected that the luminescence exhibits a high-order nonlinear response to the excitation intensity. In this measurement, we recorded luminescence images of the nanoparticles with different excitation intensities of 1550- and 980-nm light and then obtained luminescence intensities from each image. To record the luminescence images, we used a photomultiplier tube (H10722, Hamamatsu Photonics) instead of the fiber-coupled spectrometer. In luminescence imaging with a skin tissue phantom (described later), we detected both 550- and 660-nm emissions to obtain images with as high a signal-to-noise ratio (SNR) as possible. Figures 1(b) and 1(c) show double logarithmic plots of the luminescence as a function of the excitation intensity. From the slopes of linear fits in Figs. 1(b) and 1(c), we confirmed that, under 1550-nm excitation, the luminescence intensity was proportional to the 1.68th power of the excitation intensity in the low-intensity region. However, when the excitation intensity became higher than ~10 kW/cm^2, the luminescence signal started to increase almost linearly (the slope: 1.04) with the excitation intensity and then the slope finally became 0.697. In the case of 980-nm excitation, the luminescence intensity showed almost linear response (the slope: 1.06) over the entire excitation intensity range. Considering that the upconversion emission was induced via sequential two-, three-, and four-photon absorption processes, the luminescence responses were presumed to show higher order nonlinearity more clearly. The reason why the luminescence responses did not show high order nonlinearity is considered to be due to saturation effects of intermediate excited states of Er^{3+}, which have micro-to-millisecond order lifetimes, as described in Ref. 16. The luminescence lifetime changes from several hundred microseconds to submillisecond depending on Er^{3+} concentration,[18] and similar saturation effects have been reported elsewhere.[19,20] Although it was expected that high-order nonlinear responses would clearly appear if we observe UCNPs with much lower excitation intensities, a sufficiently high SNR was not achieved. The reason for the insufficient SNR is considered because we obtained the luminescence signals from luminescence images of the small-sized nanoparticles. In the previously reported studies about photoluminescence properties, much larger and brighter particles (μm-order in diameter) or microcrystals were used.[13,14,16,17] However, it is hard to use such large particles or microcrystals as luminescent probes for tissue or cellular imaging. To ensure a fair comparison of the spatial resolution in luminescence imaging with the skin tissue phantom described later, we decided to use the linear response region of the 1550-nm excitation because the luminescence response under 980-nm excitation was linear in the entire excitation intensity region.

3 Comparison of Lateral Resolution in Deep Tissue Imaging with 1550- and 980-nm Excitation

To compare the lateral resolution in deep tissue imaging, we observed nanoparticles immobilized on a coverslip through

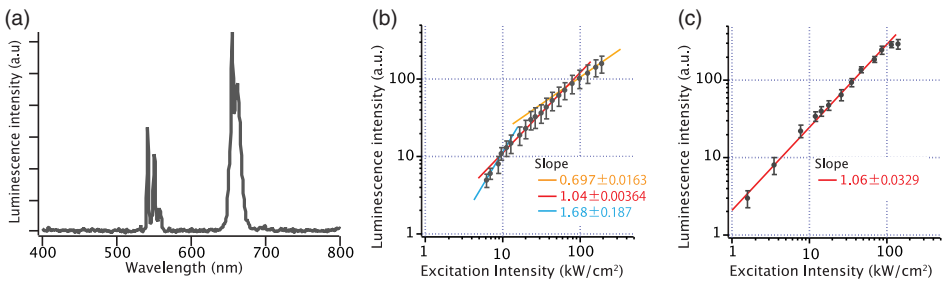

Fig. 1 (a) Luminescence spectrum of $NaYF_4$: Er, Yb nanoparticles excited by 1550-nm wavelength light and the relationship between luminescence and excitation intensity under (b) 1550 and (c) 980 nm excitation.

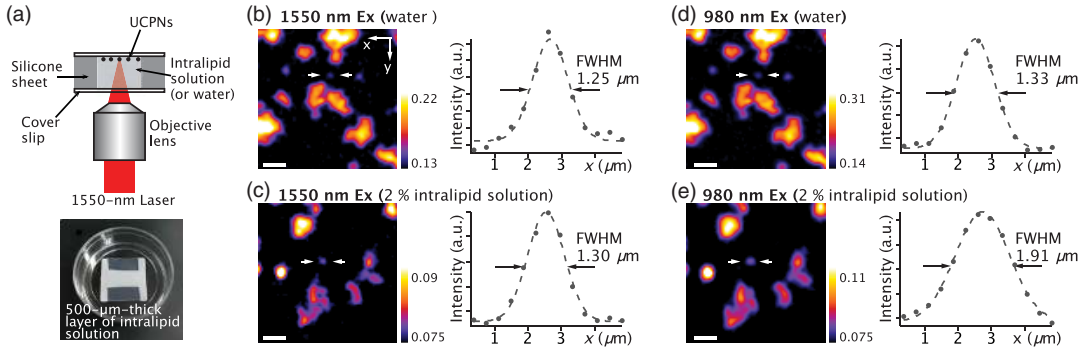

Fig. 2 (a) Schematic diagram of sample observation and photograph of 500-μm-thick layer of 2% intralipid solution. Luminescence images of UCNPs observed through a 500-μm-thick layer of water with (b) 1550 and (d) 980 nm excitation and through a 500-μm-thick layer of 2% intralipid solution with (c) 1550 and (e) 980 nm excitation. In this nanoparticle imaging, both 550 and 660 nm emissions were detected.

a skin tissue phantom. In this experiment, as the skin tissue phantom, we prepared an intralipid solution (2 v/v % intralipid and 98 v/v % H_2O) by diluting Intralipos 20% [Intralipid in H_2O (20 v/v %), Otsuka Pharmaceutical Factory] with distilled water.[21] As shown in Fig. 2(a), the thickness of the phantom was set to 500 μm by using a silicone rubber sheet. The objective lens was the same as that used for the spectral and luminescence response measurements in Fig. 1, and the working distance of the objective lens was 800 μm. In this experiment, the lateral resolutions under 1550- and 980-nm excitation were set to be almost the same by adjusting the incident beam diameters. The effective NAs for 1550- and 980-nm excitation were estimated to be ~0.75 and ~0.55, respectively. Figures 2(b) and 2(d) show luminescence images of the same nanoparticles observed with 1550- and 980-nm excitation. In this imaging, we used distilled water instead of the intralipid solution. The excitation intensities for 1550 and 980 nm were 38 and 1.6 kW/cm^2, respectively. The smallest size of a single spot in the luminescence images was chosen to compare the sizes of its intensity profiles obtained under 1550- and 980-nm excitation. As shown in the images, without scatterers in the 500-μm-thick water layer, the full-widths at half-maximum of the intensity profiles across the spot indicated by the white arrows were similar under 1550-nm excitation (1.25 μm) and 980 nm excitation (1.33 μm). To compare the effects of scattering on the lateral resolution, we replaced the water with a 2% intralipid solution and observed the nanoparticles. The excitation intensities for 1550 and 980 nm were 230 and 53 kW/cm^2, respectively. In these experiments with water and the intralipid solution, the laser intensities were calculated by using the laser power at the pupil of the objective lens, assuming a diffraction-limited focus size. The actual excitation intensities at the laser focus were presumed to be smaller than the above-mentioned intensities due to light attenuation caused by light absorption by water and scattering by the intralipid. Figures 2(c) and 2(e) show luminescence images at the same position. From these results, we confirmed that, while the image of the nanoparticles obtained with 980-nm excitation was blurred, the image obtained with 1550-nm excitation was not. The degradation percentages of the lateral resolution for 1550- and 980-nm excitation were around 4% and 40%, respectively. This result is clear evidence that the use of 1550-nm excitation moderated the degradation of the spatial resolution in deep tissue imaging. Note that, in this experiment, the effective NA was higher for focusing 1550-nm light, which is disadvantageous for preventing degradation of the spatial resolution in deep tissue imaging because larger aberrations are usually caused by the use of a higher NA objective lens.[22]

4 Live Cell Imaging with 1550-nm Excitation

Finally, we performed live cell imaging of HeLa cells cultured on a coverslip. The UCNPs were introduced into the HeLa cells by using an endocytosis reaction. We also labeled mitochondria with MitoTracker Orange (Ex/Em: 554/576 nm, M7510, ThermoFisher Scientific). To observe the mitochondria, we introduced a 532-nm CW laser source into our laser scanning microscope. In this experiment, we first took an image of UCNPs with 1550-nm excitation and then switched the excitation wavelength to 532 nm with a mirror mounted on a mechanical flipper. The excitation intensities for 1550- and 532-nm excitation were 20 and 0.6 kW/cm^2, respectively. Figure 3 shows a luminescence image of the UCNPs, a fluorescence image of mitochondria in the HeLa cells, and their merged image. This result indicated that 1550-nm excitation of Er^{3+}-doped nanoparticles is applicable to *in vitro* cellular imaging. In this experiment, we found that the nanoparticles were not introduced into all cells. The efficiency of nanoparticle transportation into cells would be improved by using additional agents, such as Lipofectamine.[23]

5 Conclusion

In this work, we demonstrated 1550-nm excitation of erbium (Er^{3+})-doped nanoparticles for upconversion luminescence bioimaging for the first time. From a comparison with the case using 980-nm excitation, which is the wavelength conventionally used for imaging UCNPs, we verified that the use of 1550-nm excitation moderated the degradation of the spatial resolution in deep tissue imaging. In addition, we also demonstrated the feasibility of live cell imaging with 1550-nm excitation of Er^{3+}-doped nanoparticles.

So far, 1550-nm excitation of Er^{3+}-doped nanoparticles has not been intensively investigated for bioimaging, although there are reports about its upconversion photoluminescence properties under 1550-nm excitation. This is presumably because absorption coefficients by water become larger in the longer-wavelength NIR region and photoinduced thermal damage is concerned in deep tissue imaging.[24] Indeed, in our deep tissue imaging experiment, 1550-nm excitation required high

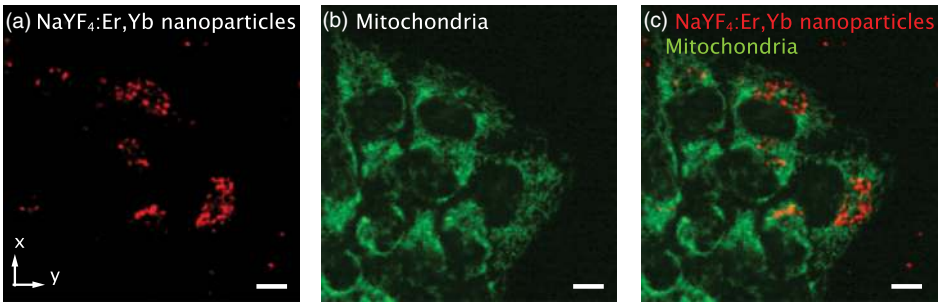

Fig. 3 (a) Luminescence image of $NaYF_4$: Er, Yb nanoparticles, (b) fluorescence image of mitochondria labeled with MitoTracker Orange, and (c) merged image of (a) and (b) (red: nanoparticles, green: mitochondria). In this nanoparticle imaging, both 550 and 660 nm emissions were detected.

excitation intensity, such as 230 kW/cm^2, to obtain a sufficiently high SNR. This high excitation intensity in 1550-nm wavelength might cause photoinduced thermal damage on tissues. However, recent studies on brain imaging with longer wavelength NIR light showed that absorbance of rat brains in the 1550-nm wavelength region is similar to that in the 1000-nm wavelength region.[15] This fact indicates that, if the brightness of Er^{3+}-doped nanoparticles under 1550-nm excitation is improved, the brightness improvement could allow us to perform deep tissue imaging with a sufficiently low excitation intensity as well as in the case of 980-nm excitation. The brightness could be improved by doping only Er^{3+} in host materials and optimizing the concentration of Er^{3+}.[25] The photoinduced thermal effects could be moderated by using a pulsed laser for excitation. The use of a pulsed laser also might help to improve the excitation efficiency, resulting in improved brightness.[26] As discussed here, further improvements of the emission brightness and excitation schemes would open up more possibilities for using 1550-nm excitation of Er^{3+}-doped nanoparticles for a wide range of biomedical studies.

Disclosures

The authors have no financial interests and no potential conflicts of interest.

Acknowledgments

This work was partially supported by the Tatematsu Foundation, the Naito Science and Engineering Foundation, and a Grant-in-Aid for Young Scientists (A) (17H04738) from the Ministry of Education, Culture, Sports, Science and Technology (MEXT), Japan.

References

1. F. Helmchen and W. Denk, "Deep tissue two-photon microscopy," *Nat. Methods* **2**, 932–940 (2005).
2. N. C. Shaner et al., "Improved monomeric red, orange and yellow fluorescent proteins derived from Discosoma sp. red fluorescent protein," *Nat. Biotechnol.* **22**, 1567–1572 (2004).
3. G. Hong, A. L. Antaris, and H. Dai, "Near-infrared fluorophores for biomedical imaging," *Nat. Biomed. Eng.* **1**, 0010 (2017).
4. A. L. Antaris et al., "A small-molecule dye for NIR-II imaging," *Nat. Mater.* **15**, 235–242 (2016).
5. S. Kim et al., "Near-infrared fluorescent type II quantum dots for sentinel lymph node mapping," *Nat. Biotechnol.* **22**, 93–97 (2004).
6. G. Hong et al., "Through-skull fluorescence imaging of the brain in a new near-infrared window," *Nat. Photonics* **8**, 723–730 (2014).
7. E. Hemmer et al., "Upconverting and NIR emitting rare earth based nanostructures for NIR-bioimaging," *Nanoscale* **5**, 11339–11361 (2013).
8. S. Fukushima et al., "Y_2O_3:Tm, Yb nanophosphors for correlative upconversion luminescence and cathodoluminescence imaging," *Micron* **67**, 90–95 (2014).
9. H. Niioka et al., "Enhancement of near-infrared luminescence of Y_2O_3: Ln, Yb (Ln = Tm, Ho, Er) by Li-ion doping for cellular bioimaging," *Chem. Lett.* **45**, 1406–1408 (2016).
10. Q. Liu et al., "Highly photostable near-IR-excitation upconversion nanocapsules based on triplet-triplet annihilation for in vivo bioimaging application," *ACS Appl. Mater. Interfaces* **10**, 9883–9888 (2018).
11. Q. Liu et al., "Single upconversion nanoparticle imaging at sub-10 W cm^{-2} irradiance," *Nat. Photonics* **12**, 548–553 (2018).
12. F. Vetrone et al., "Temperature sensing using fluorescent nanothermometers," *ACS Nano* **4**, 3254–3258 (2010).
13. L. Xinyue et al., "Blue upconversion of Tm^{3+} using Yb^{3+} as energy transfer bridge under 1532 nm excitation in Er^{3+}, Yb^{3+}, Tm^{3+} tri-doped $CaMoO_4$," *J. Rare Earths* **33**, 475–479 (2015).
14. X. Wang et al., "Up-conversion luminescence, temperature sensing properties and laser-induced heating effect of Er^{3+}/Yb^{3+} co-doped $YNbO_4$ phosphors under 1550 nm excitation," *Sci. Rep.* **8**, 5736 (2018)
15. L. Shi et al., "Transmission in near infrared optical windows for deep brain imaging," *J. Biophotonics* **9**, 38–43 (2016)
16. J. Nie et al., "Upconversion luminescence properties of different fluoride matrix materials $NaREF_4$ (RE: Gd, Lu, Y) doped with Er^{3+}/Yb^{3+}," *J. Lumin.* **204**, 333–340 (2018).
17. K. Zheng et al., "Ultraviolet upconversion fluorescence of Er^{3+} induced by 1560 nm laser excitation," *Opt. Lett.* **35**, 2442–2444 (2010).
18. Y. Ding et al., "Enhancement on concentration quenching threshold and upconversion luminescence of β-NaFY4:Er^{3+}/Yb^{3+} codoping with Li^+ ions," *J. Alloys Compd.* **599**, 60–64 (2014).
19. Y. Wang et al., "Nonlinear spectral and lifetime management in upconversion nanoparticles by controlling energy distribution," *Nanoscale* **8**, 6666–6673 (2016).
20. P. Villanueva-Delgado, K. W. Kramer, and R. Valiente, "Simulating energy transfer and upconversion in β-$NaYF_4$: Yb^{3+}, Tm^{3+}," *J. Phys. Chem. C* **119**, 23648–23657 (2015).
21. T. L. Troy and S. N. Thennadil, "Optical properties of human skin in the near infrared wavelength range," *J. Biomed. Opt.* **6**, 167–176 (2001).
22. N. Ji, "Adaptive optics fluorescence microscopy," *Nat. Methods* **14**, 374–380 (2017).
23. B. Sikora et al., "Transport of $NaYF_4$:Er^{3+}, Yb^{3+} up-converting nanoparticles into HeLa cells," *Nanotechnology* **24**, 235702 (2013).
24. S. L. Jacques, "Optical properties of biological tissues: a review," *Phys. Med. Biol.* **58**, R37–R61 (2013).
25. S. Wen et al., "Advances in highly doped upconversion nanoparticles," *Nat. Commun.* **9**, 2415 (2018).
26. H. Liu et al., "Deep tissue optical imaging of upconverting nanoparticles enabled by exploiting higher intrinsic quantum yield through use of millisecond single pulse excitation with high peak power," *Nanoscale* **5**, 10034 (2013).